Journal of Nuclear Materials 382 (2008) 39–45

Contents lists available at ScienceDirect

Journal of Nuclear Materials

journal homepage: www.elsevier.com/locate/jnucmat

Study of neodymium extraction in molten fluorides by electrochemical co-reduction with aluminium

M. Gibilaro, L. Massot *, P. Chamelot, P. Taxil

Laboratoire de Génie Chimique UMR 5503, Département Procédés Electrochimiques, Université de Toulouse, 31062 Toulouse cedex 9, France

ARTICLE INFO

Article history:
Received 4 March 2008
Accepted 4 September 2008

ABSTRACT

This work describes the co-deposition process of Al–Nd alloys in LiF–CaF_2 medium (79–21% mol) on tungsten electrode at 860 °C using electrochemical techniques: cyclic and square wave voltammetries and potentiostatic electrolyses. Specific peaks of Al–Nd alloys formation were observed in cyclic voltammograms between the reduction waves of Nd(III) and Al(III), in a fluoride melt containing neodymium and aluminium ions. The potential difference measured between the solvent reduction and the alloys formation should allow expecting an extraction efficiency of 99.99% by the use of the co-reduction process. The intermetallic compounds ($Al_{11}Nd_3$, Al_3Nd, $AlNd_2$ and $AlNd_3$) were obtained and characterised by Scanning Electron Microscopy with EDS probe. The validity of the process was tested by carrying neodymium extraction in the form of Al–Nd alloy; the extraction efficiency was more than 95%.

1. Introduction

Since 1991, French nuclear industries investigate alternative solutions for radioactive wastes treatment. Partitioning and transmutation (P&T) aim is to reduce significantly the amount of radiotoxic nuclear waste at the end of the fuel recycling. This means that the most radiotoxic elements (Pu, Am, Cm) are consumed by transmutation and that the process should have an efficient separation for actinides (An) and lanthanides (Ln). The actual hydrometallurgical process PUREX allows uranium and plutonium to be extracted for further recycling. In novel generation reactors, this process is no more available for extraction of lanthanides and actinides which exhibit too low solubility in aqueous medium. An alternative route should be the use of pyrochemical processes using molten salts, which are now used for the separation of An from Ln.

Among these techniques, the actinides recovery processes by reductive extraction on liquid metal is relevant. This extraction consists in placing in a molten solution containing the element to be extracted (MF_x) with a liquid metallic phase containing a reductive agent (A). The solute MF_x is reduced and transferred into the metal:

$$MF_{x\ (solution)} + A_{(metal)} \rightarrow M_{(metal)} + AF_{x\ (solution)}. \quad (1)$$

This extraction mode has been investigated by the following authors:

- *Chloride salts:* Kurata et al. [1] used liquid cadmium and bismuth in LiCl-KCl medium at 500 °C, or Lambertin et al. [2] a liquid gallium at 800 °C in $CaCl_2$ and NaCl–KCl media.
- *Fluoride salts:* Moriyama et al. [3] used Bi, Sn, Cd and Zn liquid metal between 600 and 800 °C in LiF–BeF_2, and Rault et al. [4] LiF–AlF_3 salts liquid aluminium at 765 °C.

According to Rault et al. [4], the best separation coefficient of An and Ln distribution in a molten fluoride salt is obtained with an aluminium-based pyrochemical system. This was confirmed by Conocar et al. [5] which demonstrated, with thermodynamic calculations in LiF–AlF_3 media at 830 °C, that aluminium is the most promising metallic solvent for the An–Ln separation. Moreover, An extraction using a liquid aluminium electrode leads to alloys formation presenting stronger interactions between An and liquid Al and thus yielding a better separation of An from Ln. Likewise, these authors [6] showed experimentally that about 99.3% of Pu and Am initially present in the melt can be recovered from a bath containing lanthanides and respecting the following scheme:

$$AnF_{3\ (solution)} + Al_{(metal)} \rightarrow An_{(metal)} + AlF_{3\ (solution)}. \quad (2)$$

This process allows keeping actinides in the Al metallic phase while lanthanides remain in the LiF–AlF_3 salt.

Further to the An–Ln separation, the Ln extraction, in presence of aluminium ions coming from the solvent and the aluminium oxidation, must be realised to recycle the molten solvent. The simultaneous presence of these two metallic ions in the melt lets up to attempt a co-reduction process which should have the advantage of extracting Al(III) and Ln(III) in a single-step, yielding Al–Ln alloys.

The present work is dedicated to the extraction of both Ln and Al elements from molten fluorides solution. The process we used is the co-reduction of Al and Ln ions yielding an alloy of these two metals. The results presented here can be used either in the frame

* Corresponding author. Tel.: +33 561 558 194; fax: +33 561 556 139.
E-mail address: massot@chimie.ups-tlse.fr (L. Massot).

0022-3115/$ - see front matter © 2008 Elsevier B.V. All rights reserved.
doi:10.1016/j.jnucmat.2008.09.004

of recovering a molten salt mixture free of Al and Ln ions for recycle Molten Salts Reactor or more generally for preparing aluminium alloy with Ln.

Neodymium is known to be the most concentrated element in the fission product [7]; so the study will be realised with neodymium as the lanthanide element.

In a first part of this article, respective reduction mechanisms of Al(III) and Nd(III) in LiF–CaF_2 on tungsten electrode earlier investigated in our Laboratory will be reminded. Then, will follow an electrochemical characterisation of the AlF_3–NdF_3 co-reduction system and analysis of Al-Nd compounds formed on the cathode will be performed by SEM. Finally, we will examine the feasibility of the extraction of Nd(III) by co-reduction process.

2. Experimental

The cell consisted of a vitreous carbon crucible placed in a cylindrical vessel made of refractory steel and closed by a stainless steel lid cooled inside by circulating water. The inner part of the walls was protected against fluoride vapours by a graphite liner containing the experimental crucible. The experiments were performed under an inert argon atmosphere (U-grade: less than 5 ppm O_2), previously dehydrated and deoxygenated using a purification cartridge (Air Liquide). The cell was heated using a programmable furnace and the temperature was measured using a chromel–alumel thermocouple. A more detailed description of the device can be found in previous papers of our laboratory such as the one referred in [8].

The electrolytic bath consisted of the eutectic LiF/CaF_2 (SDS 99.99%) mixture (79/21 molar ratio). Before use, it was dehydrated by heating under vacuum (3×10^{-2} mbar) from the room temperature up to its melting point (762 °C) for 72 h. For providing aluminium and neodymium ions, aluminium fluoride AlF_3 (SDS 99.95%) and neodymium fluoride (SDS 99.99%) powders were introduced into the bath through a lock chamber under argon gas atmosphere.

Electrochemical equipment: all electrochemical studies and electrolyses were performed with an Autolab PGSTAT 30 potentiostat/galvanostat controlled by a computer using the research software GPES 4.9.

Electrochemical techniques: cyclic voltammetry, square wave voltammetry and potentiostatic electrolyses were used for the investigation of the aluminium–neodymium co-reduction process.

Characterisation of reduction products: after electrolysis runs, cathode surface was examined by scanning electron microscopy (LEO 435 VP) equipped with an EDS probe (Oxford INCA 200) for determining the composition of the alloys.

2.1. Analytical setting

For investigations on electrochemical behaviour of the fluoride baths, we used the following cell.

Tungsten wire (1 mm diameter) was used as working electrode. The surface area of the working electrode was determined by measuring its immersion depth in the bath after withdrawing from the cell. The auxiliary electrode was a vitreous carbon rod (3 mm diameter) with a large surface area. Potentials were referred to a platinum wire (0.5 mm diameter) immersed in the molten electrolyte, acting as a quasi-reference electrode $Pt/PtO_x/O^{2-}$ [9].

2.2. Extraction setting

Compared with the previous setting, the extraction experiments need specific arrangements:

(1) The reference electrode is a nickel 1 mm diameter wire immersed in a mixture of LiF–CaF_2–NiF_2 (1 mass%), placed in a boron nitride basket. This reference electrode was proved to be reliable in molten fluoride baths [10]. Moreover, the insulation from the electrolytic bath guarantees the invariability of its potential with the change of composition of the electrolyte.
(2) The anode made of vitreous carbon was isolated in a graphite compartment containing LiCl–LiF–CaF_2 eutectic mixture. The anodic reaction was the chlorine release; the electrode compartmentalisation avoids gas and fluoride media mixing and re-oxidation of Al–Nd compounds produced at the cathode.
(3) The working electrode was a tungsten plate with a large surface area (3 cm^2).

3. Results and discussion

3.1. Co-reduction principle

The simultaneous reduction of two or several ions on an inert cathodic material was widely described by Brenner [11] and more recently by Taxil et al. [12]. One of its characteristics is the controlled-process by solutes diffusion in the bath compared to the intermetallic diffusion limitation when a reactive electrode is used. Its advantage is to provide a defined composition preventing a further variation of composition due to the intermetallic diffusion.

In the case of two metallic ions, R^{n+} and N^{p+} where R is the more reactive precursor, N the less reactive and R_xN_y the alloy formed by co-reduction, the co-reduction process occurs in three steps: (1) $xR^n + ne^- = xR$; (2) $yN^{p+} + pe^- = yN$; (3) $xR + yN = R_xN_y$.

$$\text{The overall process is } xR^{n+} + yN^{p+} + (n+p)e^- = R_xN_y. \tag{3}$$

The equilibrium potential of the system R/R_xN_y can be expressed as

$$E_{R^{n+}/R_xN_y} = E^0_{R^{n+}/R} + \frac{RT}{nF}\ln\left[\frac{a_{R^{n+}}}{a_R(\text{in } R_xN_y)}\right], \tag{4}$$

$$E_{R^{n+}/R_xN_y} = E_{R^{n+}/R} - \frac{RT}{nF}\ln\left[a_R(\text{in } R_xN_y)\right], \tag{5}$$

where $E_{R^{n+}/R}$ the equilibrium potential of pure R element, T the absolute temperature in K, n the number of exchanged electron, F the Faraday constant (96 500 C) and a_R(in R_xN_y) the activity of R in the intermetallic compound R_xN_y.

As a_R in R_xN_y is less than one, it can be deduced that $E_{R^{n+}/R_xN_y} > E_{R^{n+}/R}$.

So, the co-deposition of R with a more noble metal allows R^{n+} ions to be reduced at a potential shifted towards more positive values, compared to the pure metal deposition: this 'depolarisation effect' is similar to the one observed when the reduced element reacts with the cathode material [13].

Nevertheless, the depolarisation effect is significant only if the binary system R–N can form intermetallic compounds.

This phenomenon was earlier evidenced in the works of Wendt on TiB_2 [14] and ZrB_2 [15], who identified on cyclic voltammogram peaks of these compounds electrodeposition at potentials between pure boron and respectively pure titanium or zirconium deposition.

In the Ta–B system, Makarova et al. [16] observed a depolarisation effect of the boron potential reduction in a FLINAK melt containing boron and tantalum ions.

Electrodeposition of Sm–Co alloys was investigated in a molten LiCl–KCl–$SmCl_3$–$CoCl_2$ system at 450 °C by Iida et al. [17]. $SmCo_3$

and Sm_2Co_{17} were formed at a potential more anodic than the pure samarium deposit.

Likewise, Polyakova et al. [18] investigated for the co-deposition of titanium and niobium in a chloride–fluoride melt the behaviour of each metallic ion separately. Afterwards, these authors observed by cyclic voltammetry, when these ions are simultaneously present in the bath, the presence of a new reduction peak between the reduction of Ti and Nb ions attributed to the formation of Nb–Ti alloy.

The same methodology will be used here for the aluminium–neodymium system, knowing that the phase diagram exhibits six intermetallic compounds [19].

After summarizing the results obtained in our laboratory on the respective electrochemical behaviour of Al and Nd in fluoride solutions, the behaviour of these elements will be investigated together in molten fluorides in order to define accurately the potential of formations of intermetallic compounds.

3.2. Previous results on NdF_3 and AlF_3 reduction mechanism

The NdF_3 electrochemical reduction on inert electrode in the eutectic LiF–CaF_2 melt was investigated in our laboratory by Hamel et al. [20] and Nourry [21] and it has been stated that the reduction mechanism consists in a single-step reduction controlled by diffusion as shown on the cyclic voltammogram of the LiF–CaF_2–NdF_3 system at 860 °C on inert Mo electrode at 100 mV s^{-1} (see Fig. 1 extracted from Ref. [20]), where the peak (1 a) at −1.9 V vs. Pt is attributed to Nd(III)/Nd reduction:

$$Nd(III) + 3e^- = Nd. \quad (6)$$

Likewise, we remind the main results of our recent work on the electrochemical behaviour of AlF_3 in LiF–CaF_2 [13] which concludes that the reduction of Al(III) in Al(0) follows a single-step process exchanging 3 electrons as observed on the cyclic voltammogram of the LiF–CaF_2–AlF_3 system, at 860 °C on the W electrode at 100 mV s^{-1} presented in Fig. 2 (extracted from Ref. [13]) where only one wave of Al(III) reduction is observed:

$$Al(III) + 3e^- = Al. \quad (7)$$

3.3. Investigation of the LiF–CaF_2–AlF_3–NdF_3 system

3.3.1. Electrochemical behaviour

According to the previous results, an equilibrium potential shift of neodymium metal deposition towards the positive potential is expected for the co-reduction of Al and Nd ions into a binary Al–Nd compound where the activity of each element is less than one.

Experiments were carried out on an inert tungsten electrode at 860 °C and with the analytical setting described in Section 2.1 of the Experimental part; the electrochemical behaviour of the Al–Nd system was investigated by cyclic voltammetry and square wave voltammetry. The same metallic ions concentrations than in the individual studies above were used: [Al(III)] = 1.8 × 10^{-4} mol cm^{-3} and [Nd(III)] = 2 × 10^{-4} mol cm^{-3}. The cyclic voltammetry of this multiple system on W electrode is presented in Fig. 3. Four reduction peaks are observed:

- E_p = −1.33 V vs. Pt: this peak (2 a) is at the same potential than the one observed in Fig. 2 for the reduction of Al(III) into Al with only aluminium fluoride in the bath. Thus, it is attributed to the reduction of Al(III) in Al, while the dissolution of Al(III) in Al is observed in the reverse scan (2 b). It can be noted that the peak intensity is higher when both Al and Nd ions are present in the melt.
- E_p = −1.88 V vs. Pt: the Nd(III)/Nd system of Fig. 1 is again observed in Fig. 3 (peaks 1 a and 1 b) with a similar enhancement of the peak intensity when the two ions are simultaneously present.
- E_p = −1.49 V vs. Pt and E_p = −1.69 V vs. Pt: the additional reduction peaks (3 a and 4 a), comprised between the respective reduction potentials of Al(III) into Al and Nd(III) into Nd, should be attributed to the aluminium–neodymium co-reduction. Their respective re-oxidation peak are observed at E = −1.34 V vs. Pt (3 b) and E = −1.68 V vs. Pt (4 b).

The same distribution of peak potentials is observed in the square wave voltammogram of mixture AlF_3–NdF_3 (Fig. 4) on W electrode at 860 °C and a signal frequency of 9 Hz. The simultaneous presence of Al(III) peak (2 a), Nd(III) peak (1 a) and new peaks (3 and 4 a) of co-reduction is observed between (2 a) and (1 a).

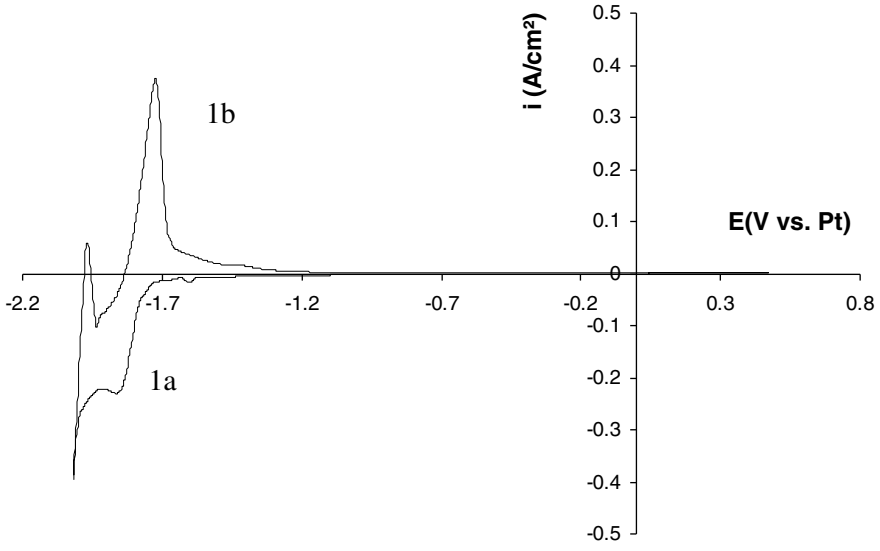

Fig. 1. Cyclic voltammogram of the LiF–CaF_2–NdF_3 (2 × 10^{-4} mol cm^{-3}) system at 100 mV s^{-1} and T = 860 °C [19]. Working electrode: W; counter electrode: vitreous carbon; quasi-reference electrode: Pt.

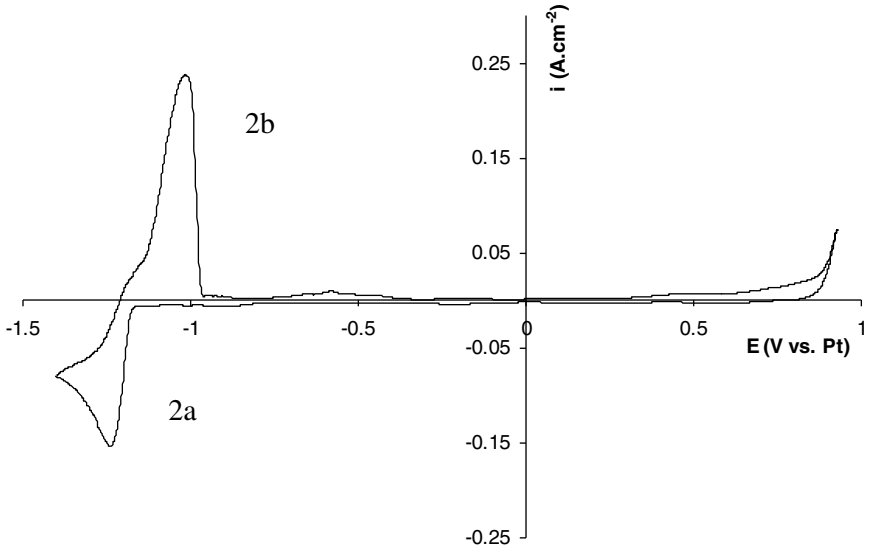

Fig. 2. Typical cyclic voltammogram of the LiF–CaF_2–AlF_3 (1.8×10^{-4} mol cm^{-3}) system at 100 mV s^{-1} and T = 860 °C [21]. Working electrode: W; counter electrode: vitreous carbon; quasi-reference electrode: Pt.

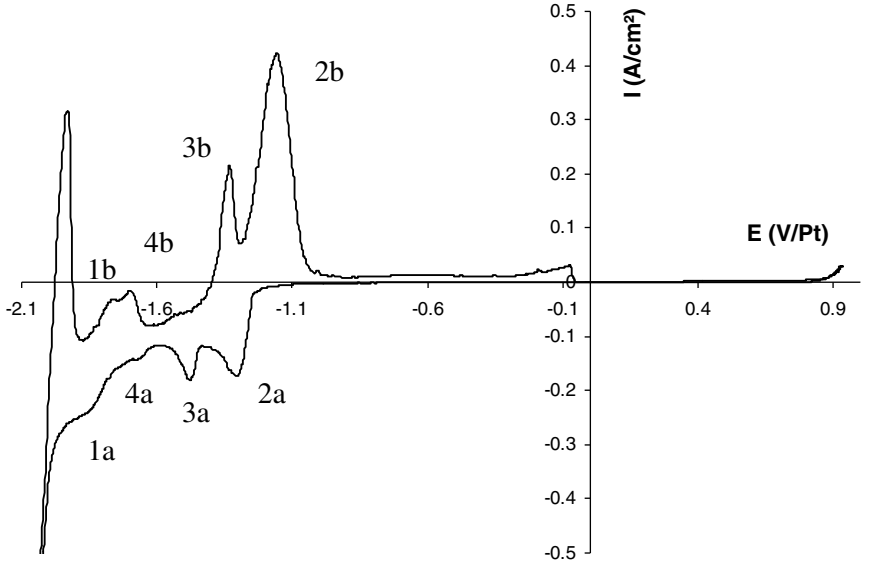

Fig. 3. Cyclic voltammogram of the LiF–CaF_2–AlF_3–NdF_3 system (respectively, 1.8×10^{-4} and 2×10^{-4} mol cm^{-3}) at 100 mV s^{-1} and T = 860 °C. Working electrode: W; counter electrode: vitreous carbon; quasi-reference electrode: Pt.

Through these preliminary observations, it can be concluded that the Al–Nd alloys co-deposition can be performed from a molten solution containing the respective metallic ions reduced together at the cathode in a potential range between the depositions of each pure metal.

3.3.2. Analysis of the co-deposition products

Potentiostatic electrolysis runs were performed on a tungsten electrode to prove that Al–Nd alloys could be produced in LiF–CaF_2 by co-reduction of the respective ions. The experimental conditions were [Al(III)] = 1.8×10^{-4} mol cm^{-3}; [Nd(III)] = 2×10^{-4} mol cm^{-3}; T = 860 °C; electrolysis time = 1200 s. Just after each run, the alloyed electrode was quenched by a rapid withdrawing from the cell. Then, an EDS analysis, joined to the SEM observation of the sample cross section, allowed us to determine all the composition phases observed on micrographs.

Electrolyses were performed with a cathode potential previously defined by cyclic voltammetry:

- E = −1.33 V vs. Pt.

The product of this electrolysis, presented in Fig. 5, exhibits only one intermetallic compound formed at the cathode, $Al_{11}Nd_3$, instead of pure Al as expected from Figs. 3 and 4. This observation leads us to conclude that at this potential Al(III) is co-reduced with Nd(III), that explains that the peak (2a) observed in Fig. 3 is higher than in Fig. 2 for similar contents in Al(III). Besides, we can note that the alloy is no adherent to the tungsten electrode.

- E = −1.49 V vs. Pt and E = −1.69 V vs. Pt.

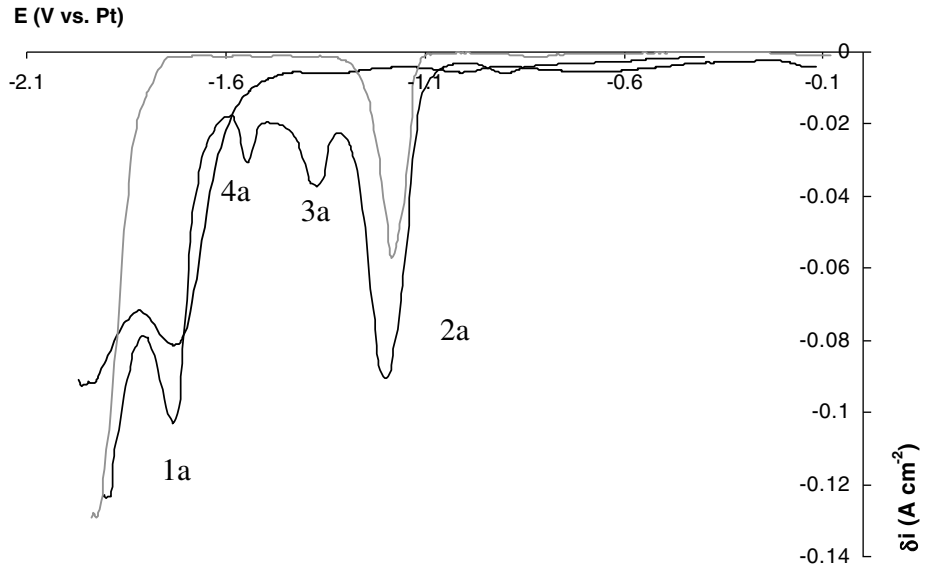

Fig. 4. Square wave voltammogram of the LiF–CaF_2–AlF_3–NdF_3 system (respectively, 1.8×10^{-4} and 2×10^{-4} mol cm^{-3}) at 9 Hz and $T = 860$ °C. Working electrode: W; counter electrode: vitreous carbon; quasi-reference electrode: Pt.

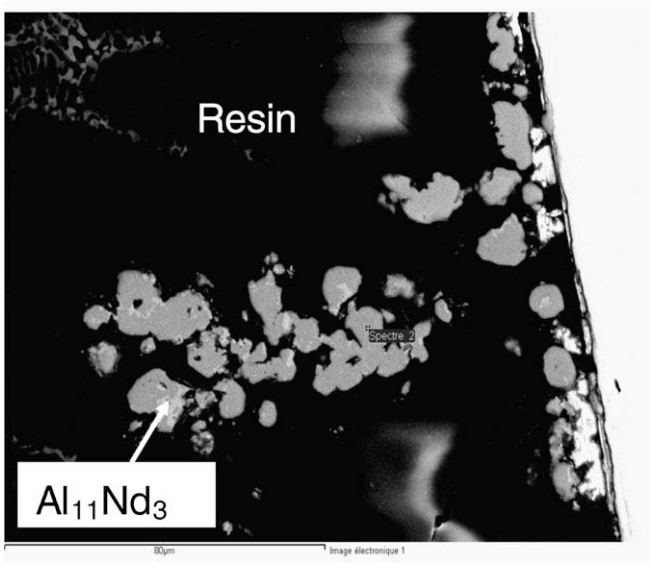

Fig. 5. Micrograph of the cross section of a tungsten wire after electrolysis. Experimental conditions: $T = 860$ °C, $E = -1.33$ V vs. Pt, $t = 1200$ s.

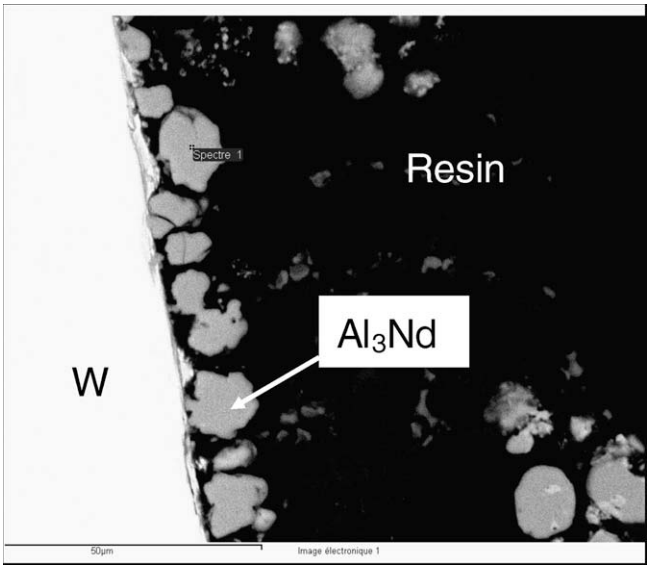

Fig. 6. Micrograph of the cross section of a tungsten wire after electrolysis. Experimental conditions: $T = 860$ °C, $E = -1.49$ V vs. Pt, $t = 1200$ s.

The electrolyses carried out at the intermediate potentials between those of pure metal electrodeposition lead to cathodic products shown in Fig. 6 (E = -1.49 V vs. Pt) and Fig. 7 (E = -1.69 V vs. Pt); both are poorly adherent and are released within the molten solution. EDS analyses prove that the composition of each of them is uniform: Al_3Nd at -1.49 V vs. Pt and $AlNd_2$ at -1.69 V vs. Pt.

- $E = -1.88$ V vs. Pt.

At this potential of pure neodymium deposition observed in Fig. 1, the electrolysis yields in Fig. 8 an intermetallic Al–Nd compound on the tungsten surface. The EDS analysis allows establishing that the product is $AlNd_3$. Once again, this result explains the enhancement of the cathodic current density observed in Fig. 4 for the reduction of Nd(III) and suggests a superimposition of a peak of Al–Nd co-reduction and pure Nd deposition.

As a general conclusion of these experiments:

(I) The aluminium–neodymium co-reduction on tungsten electrode can yield Al–Nd compounds, non adherent on the substrate and thus released in the bath.
(II) The composition of the alloys is depending on the potential of the cathode; we observe that more the electrolysis potential is cathodic, higher is the neodymium content in the intermetallic compound, as expressed in Eq. (5), where the depolarisation term is a function of the neodymium activity in the Al–Nd alloys.

3.4. Electrolytic extraction of neodymium ions by co-reduction

The following part of the work concerns the extraction of Nd(III) by co-reduction with Al(III) ions.

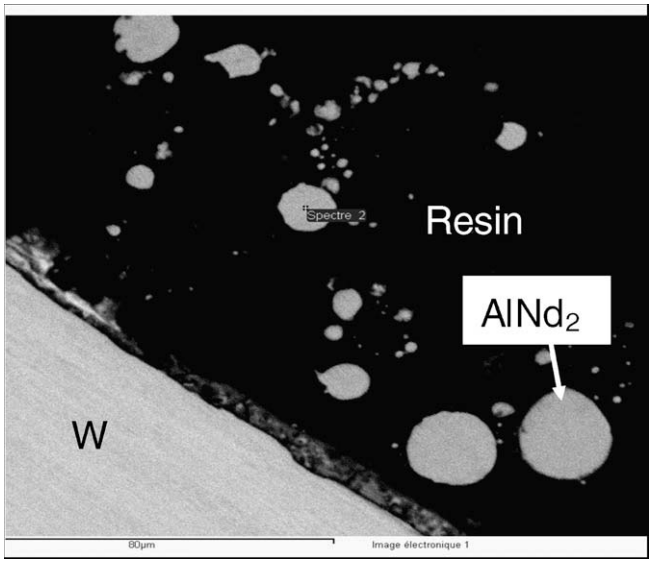

Fig. 7. Micrograph of the cross section of a tungsten wire after electrolysis. Experimental conditions: $T = 860$ °C, $E = -1.69$ V vs. Pt, $t = 1200$ s.

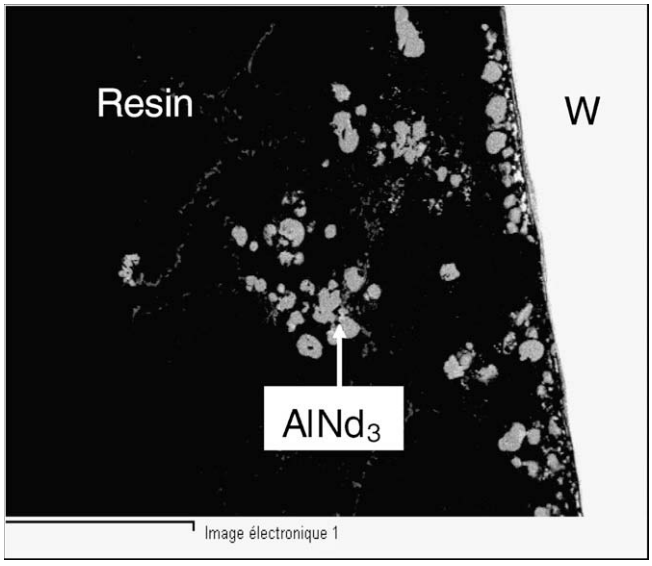

Fig. 8. Micrograph of the cross section of a tungsten wire after electrolysis. Experimental conditions: $T = 860$ °C, $E = -1.88$ V vs. Pt, $t = 1200$ s.

3.4.1. Experimental procedure

The extraction was realised on tungsten electrode in LiF–CaF_2 media at $T = 860$ °C. The initial concentrations in metallic ions were $[Al(III)] = 2.6 \times 10^{-4}$ mol cm^{-3}; $[Nd(III)] = 7.5 \times 10^{-5}$ mol cm^{-3}.

The experimental setting is described in Section 2.2 with a specific reference electrode and anodic compartment. The use of a reference electrode insulated from the electrolytic bath allows insuring the stability of the potential reference, which is essential for long time potentiostatic electrolyses runs. As the electrolysis process can sensibly change the bath composition, the platinum reference electrode immersed in the bath does not guarantee the reliability of the measured potential, whereas potentials measured with the NiF_2/Ni reference electrode remain stable. So, in the electrolysis part of the article, potentials are referred to the NiF_2/Ni electrode.

Electrolyses were performed in potentiostatic mode and the experimental procedure was the following:

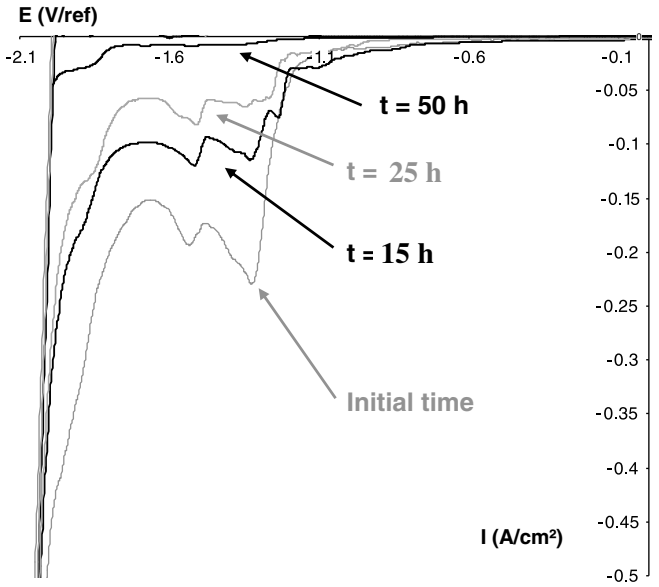

Fig. 9. Cathodic current density evolution during electrolysis measured by cyclic voltammetry. Experimental conditions: $T = 860$ °C, $v = 100$ mV s^{-1}; Working electrode: W; counter electrode: vitreous carbon; reference electrode: NiF_2/Ni.

(I) Recording of a cyclic voltammogram on a tungsten wire to choose the electrolysis potential; this potential was the co-reduction peak (3a) on the voltammogram presented in Fig. 3 in order to avoid pure neodymium deposition. The tungsten electrode was then taken out of the cell.
(II) Introduction of tungsten plate as cathode into the bath for a 3 h electrolysis time for recovering the alloy; this electrode was then withdrawn from the experimental medium.
(III) Recording a cyclic voltammogram with the W wire to measure by the signal decrease the progress of the extraction process.
(IV) These three stages are repeated as a long as an electrochemical signal, provided by the melt within the electrochemical window of the fluoride solvent, can be detected by cyclic voltammetry.

3.4.2. Neodymium aluminium co-reduction: extraction process

As mentioned above, the process was followed by drawing periodically cyclic voltammograms of the solution. Such typical voltammograms are presented in Fig. 9, where only the cathodic part is shown. A significant decrease of the current density on the cyclic voltammetry is observed, correlated to the decrease of Al(III) and Nd(III) ions concentration in the bath during the extraction process. We noticed that the current density decreased more quickly at the beginning of the electrolysis than at longer times.

Electrolyses were performed during 50 h to obtain a cathodic current density value approaching zero. The respective measurement of the current before and after the process allows the extraction rate of neodymium to be estimated at least 95%.

4. Conclusion

The possibility of preparing Al–Nd compounds by co-deposition was evidenced on the cyclic voltammogram of the Al–Nd fluoride solutions: specific electrochemical systems for the co-reduction of Al(III) and Nd(III) ions were identified in the potential range between pure Al and Nd metals deposition. Each of the four reduction waves observed are correlated to Al–Nd intermetallic compounds, further identified with SEM observation and EDS analysis after a

short electrolysis run: $Al_{11}Nd_3$, Al_3Nd, $AlNd_2$ and $AlNd_3$ were obtained on a tungsten electrode. When increasing cathodic potential, these compositions are in agreement with Eq. (5), where more the electrolysis potential is cathodic, higher is the neodymium content in the alloy.

So, these preliminary experiments have shown that it is possible to extract both neodymium and aluminium ions present in the melt at potential comprised between the equilibrium potentials of each metal.

Furthermore, a new experimental setting for the extraction has been developed and tested successfully and lead to an extraction efficiency of Nd(III) estimated to be at least 95%.

This work has shown that a novel process for lanthanides extraction based on the co-reduction between Al(III) and Nd(III) ions can be proposed. This method presents the advantage to eliminate simultaneously the two metallic ions in order to recycle the fluoride solvent.

Indeed this co-reduction process can be extended to other electrochemical systems. Thus, in a more general aspect, this work appears as a promising route for preparing intermetallic compounds involving aluminium and lanthanides.

Acknowledgements

The authors express their thanks to the PCR RSF Thorium and GDR Paris from the PACE program for financial support of this work.

References

[1] M. Kurata, Y. Sakamura, T. Hijikata, K. Kinoshita, J. Nucl. Mater. 227 (1995) 110.
[2] D. Lambertin, S. Ched'homme, G. Bourges, S. Sanchez, G.S. Picard, J. Nucl. Mater. 341 (2005) 131.
[3] H. Moriyama, T. Seshimo, K. Moritani, Y. Ito, T. Mitsugashira, J. Alloys Compd. 213&214 (1994) 354.
[4] L. Rault, M. Heusch, M. Allibert, F. Lemort, X. Deschanel, R. Boen, Nucl. Technol. 139 (2002) 167.
[5] O. Conocar, N. Douyere, J. Lacquement, J. Nucl. Mater. 344 (2005) 136.
[6] O. Conocar, N. Douyere, J.P. Glatz, J. Lacquement, R. Malmbeck, J. Serp, Nucl. Sci. Eng. 153 (2006) 253.
[7] J.P. Ackerman, Ind. Eng. Chem. Res. 30 (1) (1991) 141.
[8] P. Chamelot, P. Taxil, B. Lafage, Electrochim. Acta 39-17 (1994) 2571.
[9] A.D. Graves, D. Inman, Nature 208 (1965) 481.
[10] P. Taxil, Z. Qiao, J. Chim. Phys. 82 (1) (1985) 83.
[11] A. Brenner, Electrodeposition of Alloys, vol. 1, Academic Press, New York, 1963.
[12] P. Taxil, P. Chamelot, L. Massot, C. Hamel, J. Min. Met. 39 (2003) 177.
[13] M. Gibilaro, L. Massot, P. Chamelot, P. Taxil, J. Alloys Compd. (2008). doi:10.1016/j.jallcom.2008.03.115.
[14] H. Wendt, K. Reuhl, V. Schwarz, Electrochim. Acta 37 (2) (1992) 237.
[15] H. Wendt, K. Reuhl, V. Schwarz, J. Appl. Electrochem. 22 (1992) 161.
[16] O.V. Marakova, L.P. Polyakova, E.G. Polyakov, A.A. Shevyryov, A.V. Arakcheeva, J. Min. Met. 39 (2003) 261.
[17] T. Iida, T. Nohira, Y. Ito, Electrochim. Acta 48 (2003) 2517.
[18] L.P. Polyakova, P. Taxil, E.G. Polyakov, J. Alloys Compd. 359 (2003) 244.
[19] H. Okamoto, T.B. Massalski, J. Phase Equilibria 12 (2) (1991) 148.
[20] C. Hamel, P. Chamelot, P. Taxil, Electrochim. Acta 49 (2004) 4467.
[21] C. Nourry, Extraction Electrochimique des Lanthanides des Milieux Fluorures Fondus par Formation d'Alliage, PhD Thesis, Toulouse, 2007.